

Rouser: Robust SNN training using adaptive threshold learning

Sanaz M. Takaghaj, Jack Sampson

Abstract. In Spiking Neural Networks (*SNNs*), learning rules are based on neuron spiking behavior, that is, if and when spikes are generated due to a neuron’s membrane potential exceeding that neuron’s firing threshold, and this spike timing encodes vital information. However, the threshold is generally treated as a hyperparameter, and incorrect selection can lead to neurons that do not spike for large portions of the training process, hindering the effective rate of learning. Inspired by homeostatic mechanisms in biological neurons, this work (*Rouser*) presents a study to rouse training-inactive neurons and improve the SNN training by using an in-loop adaptive threshold learning mechanism. Rouser’s adaptive threshold allows for dynamic adjustments based on input data and network hyperparameters, influencing spike timing and improving training.

This study focuses primarily on investigating the significance of learning neuron thresholds alongside weights in SNNs. We evaluate the performance of Rouser on the spatiotemporal datasets NMNIST, DVS128 and Spiking Heidelberg Digits (SHD), compare our results with state-of-the-art SNN training techniques, and discuss the strengths and limitations of our approach. Our results suggest that promoting threshold from a hyperparameter to a parameter can effectively address the issue of dead neurons during training, resulting in a more robust training algorithm that leads to improved training convergence, increased test accuracy, and substantial reductions in the number of training epochs needed to achieve viable accuracy. Rouser achieves up to 70% lower training latency while providing up to 2% higher accuracy over state-of-the-art SNNs with similar network architecture on the neuromorphic datasets NMNIST, DVS128 and SHD.

1. Introduction

Neuromorphic computing is inspired by biological neural networks, which are known for their high energy efficiency in processing stimulus signals and communication. The emergence of DVS cameras, also referred to as “silicon retina” [1] and “silicon cochlea” devices [2], coupled with the use of implementable, dense on-chip artificial synapses [3, 4, 5], has propelled the field of neuromorphic engineering towards end-to-end event-based models where the data from event-based input devices would be processed via Spiking Neural Networks (*SNNs*) mapped on neuromorphic hardware fabrics. SNNs, in their general form, are composed of Leaky Integrate and Fire (LIF) neurons that have states, and, compared to conventional Artificial Neural Network (*ANNs*), more closely

mimic biological neural networks. LIF neurons are standard neuron models that can be efficiently simulated. SNNs distribute data in the temporal domain rather than the activation amplitude and, when implemented effectively, they will have lower overall memory usage. Beside having state variables (synaptic response current and membrane potential), SNNs also incorporate time as another parameter in their computations. Neuron dynamics and threshold levels specify the timing of spike generation. Since these spikes are sparse, discrete, 0/1 events, SNNs are more energy efficient in their computation, and can be implemented in extremely low-power neuromorphic hardware with low memory access frequency requirements [6, 7, 8, 9, 10]. Many domains, from UAVs to robotics, surveillance and monitoring [11, 12, 13, 14, 15] are poised to benefit from the success of this endeavor.

However, a key roadblock remains for this SNN vision of the future: SNN training is not as mature or reliable as ANN training. Bio-plausible unsupervised training algorithms, such as Hebbian learning and Spike Timing Dependent Plasticity (STDP) [16, 17], excel at extracting low-level features but often face challenges with generalization and scalability, limiting their application to shallow SNNs [18, 19]. In Reinforcement Learning, synaptic weights are subjected to random perturbations to gauge changes in output error [20, 21]. If the error decreases, the alteration is accepted; otherwise, it is rejected. With large networks, reinforcement learning becomes challenging because the effect of adjusting one weight is overshadowed by noise from others, necessitating numerous trials for meaningful learning. Due to the remarkable success of error backpropagation in training ANNs, most recent strategies for training SNNs prominently leverage gradient calculations and error backpropagation, achieved through either converting pre-trained ANNs to SNNs [22, 23, 24, 25] or directly training SNNs via modified backpropagation [24, 26, 27, 28, 29, 30, 31]. The conversion of a pre-trained non-spiking ANN into an SNN involves a trade-off between accuracy, latency and computational efficiency. And these methods are suited for static datasets where temporal dynamics are absent. Directly applying error backpropagation to SNNs is however challenging due to the non-differentiable nature of spiking neurons. To address this issue, surrogate gradients [30, 32, 33] are used to approximate the spike activation derivative as a continuous function, enabling end-to-end training of SNNs.

Neurons in SNNs have hyperparameters that control their behavior and dynamics: the firing threshold, membrane time constant (τ), and neuron update time steps. These hyperparameters are bio-inspired, and adjusting them fine-tunes neuron and network behavior. We utilize spiking neuron dynamics in both the forward and backward paths to directly train SNNs using error backpropagation on spatiotemporal datasets that incorporate a time domain. When exposed to input changes (spikes), neurons adapt their membrane potentials in response, while retaining their states in the absence of such stimuli. As a result, we determine neuron update time steps based on the time dimension in the dataset. In addition, we maintain a consistent time constant (current and voltage decays) throughout the training process, while enabling the neurons to learn the optimal threshold levels. Spiking threshold is a crucial hyperparameter with

respect to the silence or activity of a neuron, determining the level of input a neuron must receive before it can generate an output spike. It acts as a gate for the flow of data in the network. Determining optimal firing threshold levels that allow neurons to emit enough spikes and, in some cases, precisely timing their emission is a critical task in training SNNs, affecting training convergence rate, inference latency, and accuracy. Increasing the threshold can result in more precise coding of information, with only the most salient features represented by spikes. Decreasing the threshold can lead to more distributed coding, with more neurons contributing to the representation of each input feature. In backpropagation-based SNN training, achieving the right balance is crucial to avoid the “dead neuron” problem: when no neurons spike during the presentation of an input or input batch, no learning occurs under many learning rules [27, 28, 30]. The existence of dead neurons during training, particularly in the outer layer, can impede the backpropagation of the error, potentially hindering the training process and overall network performance which can lead to inefficient training and suboptimal results as reported in [26].

In SNNs, while activation sparsity is a desirable and expected property of the network, in order for gradients to backpropagate, there needs to be a sufficient pool of active neurons during training. Importantly, while “dead” neurons can be pruned from already trained networks, there is little way of knowing, during training, if a given neuron will remain inactive throughout training or is merely “comatose” and will (eventually) begin firing in future training epochs. The effectiveness of any SNN training algorithm is therefore sensitive to the specification of threshold values for neurons, and appropriate threshold values for a given topology/dataset are often discovered through offline grid search; for the same network architecture, different threshold values may be needed to have viable training for different datasets. Thus, in addition to its relationship with dead neurons, threshold is a key hyperparameter for learning robustness regardless of input inhomogeneity and initialization of weight parameters. Further, even if the current thresholds are viable for the training data seen so far, there is no guarantee that the current threshold settings will lead to desirable training outcomes if there are distributional shifts (e.g. in post-deployment training/tuning scenarios).

To address neurons that appear “dead” during training and related robustness challenges, we propose **Rouser** to extend existing backpropagation techniques and incorporate an in-loop threshold adaptation feature, which “rouses” the “dead” neurons and speeds up the training and enhances the inference accuracy. Rouser is a robust training algorithm that adjusts threshold levels for each neuron based on the membrane potential and the gradient of the output. This allows each neuron to emit sufficient spikes and contribute to the overall output gradients. In Rouser, the spiking threshold is considered as a *dynamically learnable* hyperparameter that can be adjusted according to the sparsity of incoming spikes and the threshold gradients can vary in both directions, allowing for more precise adjustments.

While feedforward networks typically reach high test accuracy after 20 training epochs [34], even starting from sub-optimal hyperparameter initialization, Rouser can

achieve the same level of accuracy in as few as 6 epochs. Due to its robust and adaptive nature, Rouser achieves up to 30% training speed-up (in terms of epochs before convergence) and up to 2% higher accuracy when compared to state-of-the-art SNN models with similar network architecture on neuromorphic datasets NMNIST, DVS128 and Spiking Heidelberg Digits (SHD). This work’s contributions include:

- An adaptive mechanism to regulate neuron activity in SNNs trained via spatiotemporal error backpropagation on neuromorphic datasets.
- An in-depth analysis of learning dynamics and the “dead neuron” problem in SNN training with gradient-based error backpropagation.
- A quantitative demonstration of inference latency and accuracy improvement attributable to threshold learning.

2. Related work

Biological neurons exhibit a phenomenon known as homeostatic plasticity [35]. This mechanism allows neurons to maintain stability and regulate their firing rates. When a neuron consistently fires too frequently/infrequently, it can adapt its threshold to achieve a more balanced firing rate.

Several methods have been explored to incorporate homeostatic plasticity into artificial neural networks. One notable approach involves the use of adaptive spiking neuron models [36, 37, 38] or Spike Frequency Adaptation (SFA) mechanisms [39]. In this context, the threshold is increased after each emitted spike, followed by an exponential decay. These techniques are used to transiently increase the neuron’s firing threshold, thus reducing the neuron’s firing rate over time. A comparable strategy is found in the threshold regularization method [30]. Here, neurons that respond to input spikes by firing have their thresholds incremented. Subsequently, for all neurons, the threshold is diminished. This approach makes highly active neurons less responsive to input stimuli due to the elevation of their thresholds, while less active neurons can more easily react to subsequent stimuli. The threshold annealing technique [40] increases the threshold level over time, using a small threshold in early epochs and a larger threshold in later epochs. Since this method always increases the threshold level without considering changes in output error, its effectiveness in achieving optimal threshold levels and eliminating inactive neurons is limited. Additionally, some methods like activity regularization [26, 33] have proposed lower bound and higher bound values on the neuronal spike counts to control spiking activity levels in SNNs. Unlike activity regularization techniques, Rouser does not enforce any constraints on neuron activities; instead, it dynamically adjusts the threshold to minimize loss function, thereby regulating neuron activities in an adaptive manner.

Another category of methods focuses on determining optimal threshold values similar to ours. The threshold balancing method [25, 23] employs a grid search of thresholds to find the best threshold values for ANN to SNN conversion. The threshold

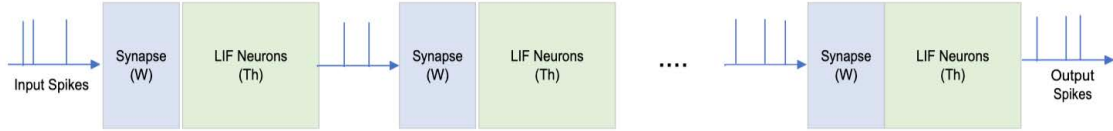


Figure 1: SNN with adjustable synaptic weights (W) and firing thresholds (Th)

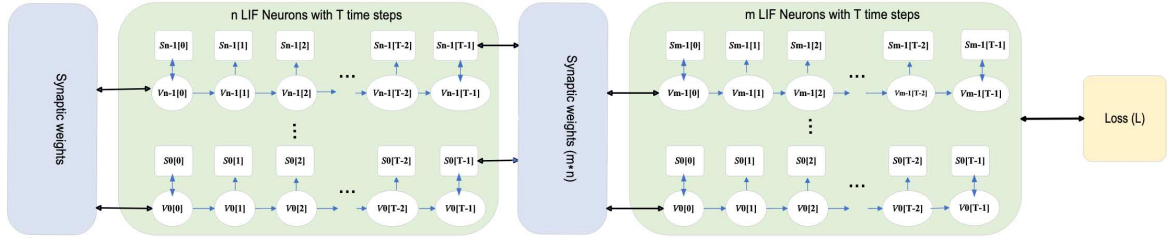


Figure 2: Illustration of our SNN topology with spatiotemporal Backpropagation. The membrane potential of each neuron $V_i(t)$ updates every discrete time step $t \in \{0, 1, \dots, T - 1\}$ for a finite number of events T . After the final layer, a loss function calculates the difference between the output spikes and the target spike train for a given input.

optimization technique [24] utilizes gradient descent to optimize the membrane time constant (leakage) and threshold values in models derived from ANN to SNN conversion. [41] uses a hyperbolic tangent function to model the threshold, constraining it within the range (-1, 1) to facilitate its incorporation into error backpropagation training on DenseNet architecture. [42] and [36] have incorporated learnable membrane time constants, demonstrating that this integration reduces sensitivity to initial values and accelerates learning within the network.

In this work, our primary focus is on the development of a computationally efficient adaptive algorithm for training feedforward SNNs on various neuromorphic (non-static) datasets. Note that our approach does not impose any limit on the thresholds, thus allowing for a greater flexibility in model optimization.

3. SNN Training using spatiotemporal backpropagation and threshold learning

In this section, we first describe the dynamics of Leaky Integrate-and-Fire (LIF) neurons [43]. A LIF neuron i has two state variables: a synaptic response current $I_i^l[t]$ and a membrane potential $V_i^l[t]$. The synaptic response current is generated by a leaky integrator which integrates the incoming spikes from a stimuli $S_j^{l-1}[t]$. This current then passes through another leaky integrator to produce the membrane potential $V_i^l[t]$.

When the membrane potential reaches a firing threshold level Th_i , the neuron sends out a spike $S_i^l[t]$ and then resets to V_{rest} . The dynamics of LIF neuron i in layer l can be described using the following equations:

$$I_i^l[t] = \frac{1}{\tau_i} I_i^l[t-1] + \sum_j w_{ji} S_j^{l-1}[t-1] \quad (1)$$

$$V_i^l[t] = \frac{1}{\tau_v} V_i^l[t-1] + I_i^l[t-1] - Th_i S_i^l[t-1] \quad (2)$$

where w_{ji} is the synaptic weights from neuron j to neuron i . The last term in (2) is to reset the membrane potential state by subtracting the threshold Th_i after spike $S_i^l[t-1]$ emission. A unit step function models the spiking function:

$$S_i^l[t] = \begin{cases} 1, & \text{if } V_i^l[t] \geq Th_i \\ 0, & \text{otherwise} \end{cases} \quad (3)$$

The spiking function $S_i^l[t]$ is non-differentiable and poses a problem for gradient calculations in error backpropagation. To overcome this issue, we use a surrogate function [33, 32] to approximate the derivative of the spiking function. We used the following functions for the surrogate gradients:

$$\frac{dS_i^l[t]}{dV_i^l[t]} = \frac{s}{\tau} e^{-\frac{|V_i^l[t]-Th_i|}{\tau}} \quad (4)$$

$$\frac{dS_i^l[t]}{dTh_i} = -\frac{s}{\tau} e^{-\frac{|V_i^l[t]-Th_i|}{\tau}} \quad (5)$$

where s is a scaling factor, and τ is the steepness parameter ($\tau \rightarrow 0$). It is worth mentioning that the derivative is larger when the membrane potential is closer to the threshold Th_i and zero when the neuron is “dead” or not firing. This means that active neurons have a greater influence on the gradient and thus play a critical role in the successful training of SNNs.

Establishing connections between these LIF neurons constructs a network. Figure 1 illustrates a simplified spiking neural network with three neurons. Each neuron is composed of synapses with associated synaptic weights $W = [w_{ji}]$ and adjustable firing thresholds $Th = [Th_i]$. Larger networks have an increased number of neurons within each layer that are connected to the neurons in the subsequent layer, forming a fully connected architecture. Figure 2 depicts a simplified model of Rouser, featuring only two layers.

We present a learning rule for training SNNs that involves adjusting the threshold of each individual neuron. We frame the training of SNNs as an optimization problem where we minimize the van Rossum distance [44] between the network’s output spikes $S[t]$ and the desired target spikes $\hat{S}[t]$ in (6). The learning rule is derived by solving this optimization problem using gradient descent:

$$L = \frac{1}{2} \int_T (H * (S[t] - \hat{S}[t]))^2 dt \quad (6)$$

where $H * (S[t] - \hat{S}[t])$ is the output error, H represents a second order Finite Impulse Response (FIR) filter which is easy to implement both computationally and in neuromorphic hardware [45, 46].

We first calculate the gradient of L with respect to V_i^l and Th_i , and then use the chain rule to find the update rules for the synaptic weights w_{ji} and the thresholds Th_i respectively:

$$\frac{\partial L}{\partial V_i^l} = \int_T (H * (S[t] - \hat{S}[t]))(H * \frac{\partial S[t]}{\partial V_i^l})dt \quad (7)$$

$$\frac{\partial L}{\partial Th_i} = \int_T (H * (S[t] - \hat{S}[t]))(H * \frac{\partial S[t]}{\partial Th_i})dt \quad (8)$$

$$w_{ji} = w_{ji} - lr_w * \frac{\partial L}{\partial V_i^l[t]} * \frac{\partial V_i^l[t]}{\partial w_{ji}} \quad (9)$$

$$Th_i = Th_i - lr_{Th} * \frac{\partial L}{\partial Th_i} \quad (10)$$

The learning rate for synaptic weights is denoted as lr_w , while the learning rate for thresholds is lr_{Th} . These learning rates can be the same or can be adjusted adaptively for each parameter, a technique commonly used in optimization algorithms like Adam [47] or RMSprop [48].

4. Experimental Results

This section analyzes applying Rouser to the neuromorphic datasets NMNIST, DVS128 and SHD. The NMNIST dataset is a spiking version of the MNIST dataset, where spikes are generated by displaying images on a neuromorphic vision camera equipped with ATIS (Asynchronous Time-based Image Sensor) [49]. It contains 60,000 training images, each consisting of 300 time samples, and an additional set of 10,000 test images used to evaluate accuracy. The DVS128 dataset, which is an event-based dataset captured using the Dynamic Vision Sensor (DVS) camera, comprises recordings of 11 hand gestures. It consists of approximately 20,000 to 40,000 events per gesture class. The dataset includes 1176 samples with varying temporal dimension allocated for training and 288 samples designated for testing [50]. The SHD dataset is an audio-based dataset consisting of spoken digits ranging from zero to nine in both the English and German languages. The audio waveforms have been converted into spike trains using an artificial model of the inner ear. The SHD dataset comprises 8,156 training samples and 2,264 test samples with varying time spans [51].

We utilized SLAYER 2.0 from Lava-DL library [54] as the baseline (control) for training SNNs with error backpropagation, employing a fixed threshold for spike generation. SLAYER 2.0 is a modified version of SLAYER [28] which is a method of training SNNs that can simultaneously learn both synaptic weights and axonal delay. In this study, we employed SLAYER 2.0 for comparative analysis; however, the analysis can be extended to any backpropagation-based approach in the training of SNNs.

Table 1: Benchmarking results

Dataset	Training Method	Threshold adj. method	Architecture	Accuracy
NMNIST	Sparse BP [26]	Regularization	34x34-200-200-10	92.7%
	SKIM [52]	–	34x34x2-10000-10	92.87%
	DART [53]	–	DART	97.95%
	Backpropagation [30]	Regularization	34x34x2-800-10	98.66%
	SLAYER [28]	–	34x34x2-500-500-10	98.89%
	ROUSER	Adaptive	34x34x2-500-500-10	99.21%
DVS128	SLAYER 2.0 [54]	–	128x128x2-64-11	84.72%
	ROUSER	Adaptive	128x128x2-64-11	86.46%
SHD	Sparse BP [26]	Regularization	700-200-200-20	77.5%
	ROUSER	Adaptive	700-200-200-20	78.14%

Table 2: Rouser’s hyperparameters

Symbols	Description	Value
T_{init}	initial threshold	1.25, 0.25
$\frac{1}{\tau_i}$	current decay	0.75
$\frac{1}{\tau_v}$	voltage decay	0.97
τ	steepness parameter	3.75, 3
s	scaling factor	1.5, 3
lr	learning rate	0.001
-	optimizer	Adam
-	weight initialization	Kaiming

Our constructed SNN consists of either two layers (for DVS128) or three layers (for NMNIST and SHD), designed to mitigate overfitting and maintain consistency with SLAYER 2.0 architecture. Additionally, we maintained uniformity in network parameters, initialization scheme and loss functions across experiments to ensure a fair comparison. The output layer includes 10 neurons for NMNIST, 11 neurons for DVS128 and 20 neurons for SHD, each corresponding to a specific output class. For NMNIST, the first two layers consist of 500 LIF neurons, while for DVS128, the first layer has 64 LIF neurons. In the case of SHD, the first two layers are configured with 200 neurons. Table 1 presents the network architecture along with the accuracy of Rouser compared to state-of-the-art results on neuromorphic datasets NMNIST, DVS128 and SHD using feedforward networks. In this study, we developed a computationally efficient algorithm for training SNNs with adaptive threshold that could be applied to diverse datasets, rather than specifically achieving the highest benchmark accuracy for a given dataset. On the DVS128 dataset, Amir et al. [50] achieved an accuracy of 94.59% with a pre-trained 16-layer CNN model, while SLAYER attained 93.64% accuracy using an 8-layer



Figure 3: Neuron’s threshold level (Th) impacts inference accuracy in SNNs. Among the tested thresholds for NMNIST, a threshold of 1 produces the highest inference accuracy after 10 epochs. For DVS128, this value is 0.75.

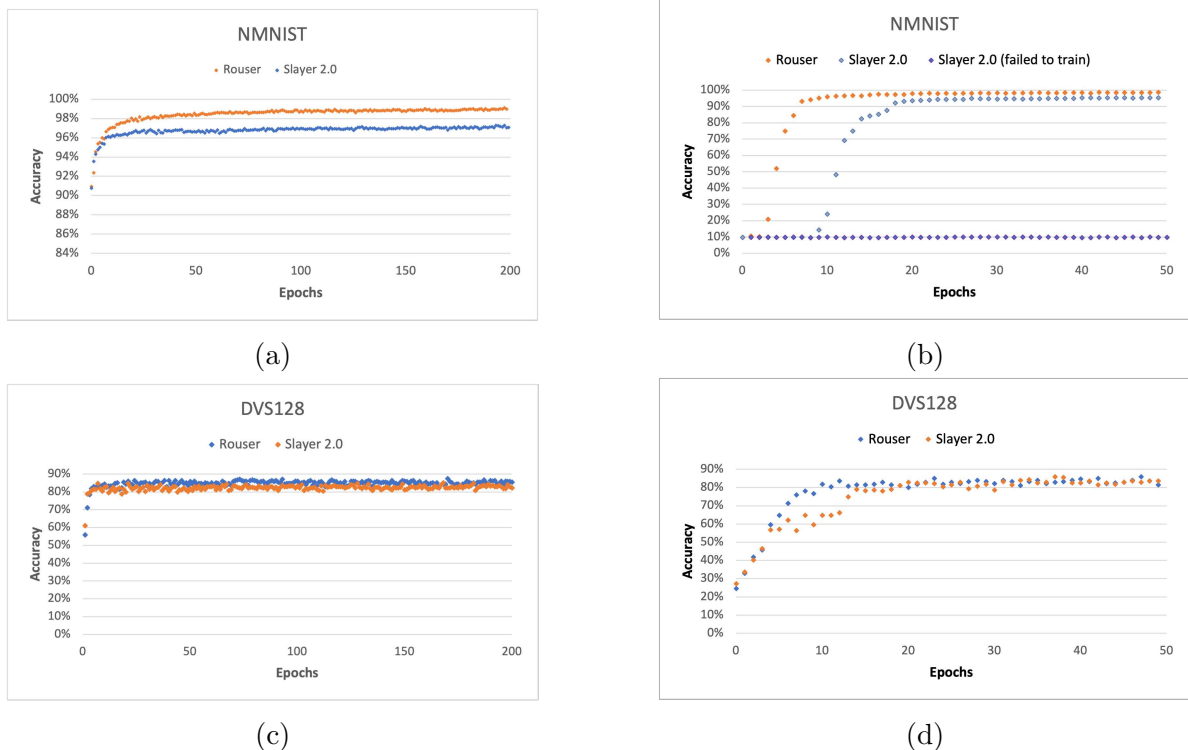


Figure 4: In a close comparison between Rouser and the baseline (SLAYER 2.0), Rouser exhibits higher accuracy and lower latency for sub-optimal hyperparameters (Th_{init} , τ , s) = (1.25, 3.75, 1.5) in (a) and (c), and (0.25, 3, 3) in (b) and (d).

CNN model [28].

To assess the impact of various threshold levels on the training of SNNs through error backpropagation, we first conducted an experiment using both the NMNIST and DVS128 datasets, systematically varying the threshold values for evaluation while keeping all other hyperparameters and the loss function constant. Our findings,

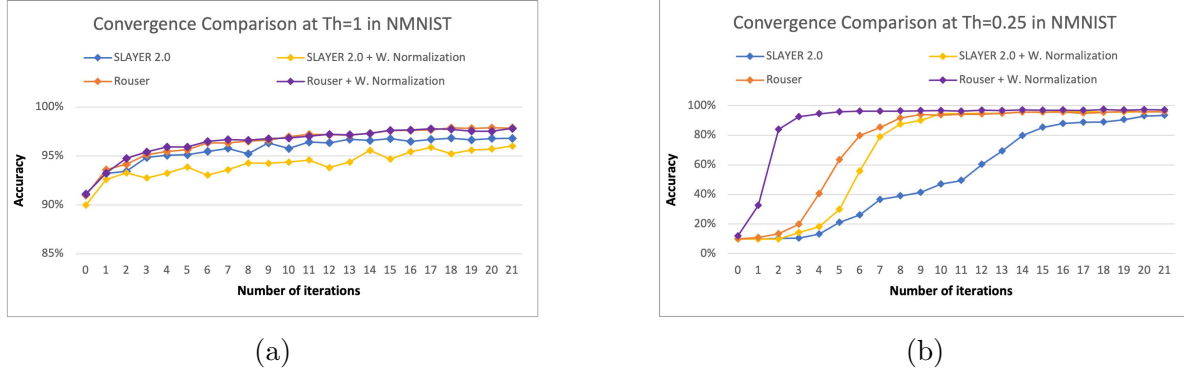


Figure 5: When the threshold is sub-optimal, backpropagation-based training methods such as SLAYER 2.0 may substantially degrade. Rouser exhibits faster training convergence when compared to both SLAYER 2.0 and SLAYER 2.0 with the addition of weight normalization technique.

illustrated in Figure 3 for both MNIST and DVS128 datasets, indicate that SNN training through error backpropagation is highly sensitive to the threshold level, and the optimal threshold value differs between these two datasets. After 10 epochs of training, we obtained a test accuracy of 96% on the MNIST dataset by setting a constant firing threshold of 1. However, when the threshold was set to 0.25, the performance of the SNN significantly deteriorated, resulting in a subpar test accuracy of 41%. Similarly, for the DVS128 dataset, we observed an accuracy of 86% when the firing threshold was set to 0.75. For a threshold of zero, the accuracy dropped to 68% (Figure 3).

We also conducted analysis studies on sub-optimal scenarios using the same loss function and initial set of hyperparameters (as in Table 2). Figure 4 shows the results. Due to Rouser’s robustness to variations in weight initialization and hyperparameters, we observed a substantial enhancement in the training convergence latency (70%) and accuracy (2%), as demonstrated in Figures 4b and 4a respectively. When the threshold is sub-optimal, backpropagation-based training methods such as SLAYER 2.0 could become unstable and may fail to effectively train the network. Figures 4c and 4d show the results of the same experiment using the DVS128 dataset.

Figure 5 compares the training convergence for two threshold values between Rouser and SLAYER 2.0, including the impact of enabling weight normalization. Weight normalization decouples the length of weight vectors from their direction, reparameterizing each weight vector w in terms of a parameter vector v and a scalar parameter g , and performs gradient descent with respect to these parameters instead. This improves the condition of the optimization problem and speeds up the convergence of Stochastic Gradient Descent (SGD) [55].

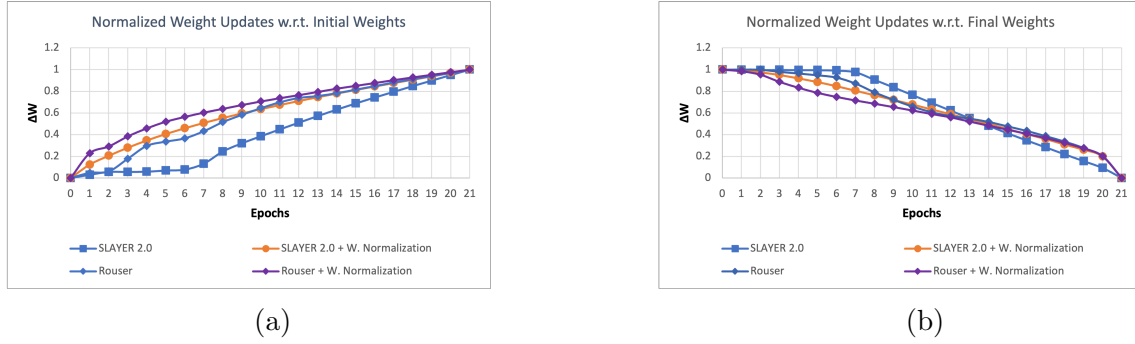


Figure 6: Weight updates with respect to initial and final weights during SNN training. Rouser has higher convergence rate than SLAYER 2.0, resulting in lower latency

4.1. Rouser’s Training Dynamic

To better understand the effectiveness of Rouser in training SNNs and gain insights into the convergence rate and stability of the network, we monitored synaptic weight and threshold changes during training. Figure 6a shows the changes in synaptic weights over time compared to the initial weights, while Figure 6b shows the weight changes over time compared to the settled weights. In figure 6a, we observed that Rouser has higher weight changes than SLAYER 2.0 indicating faster training and a lower latency. In contrast, SLAYER 2.0 showed comparatively lower weight changes and longer training times. Figures 7 and 8 illustrate the variations in threshold values over time for the NMNIST and DVS128 datasets respectively. Rouser dynamically determines the optimal threshold values for each epoch, leading to reduced latency and improved test accuracy.

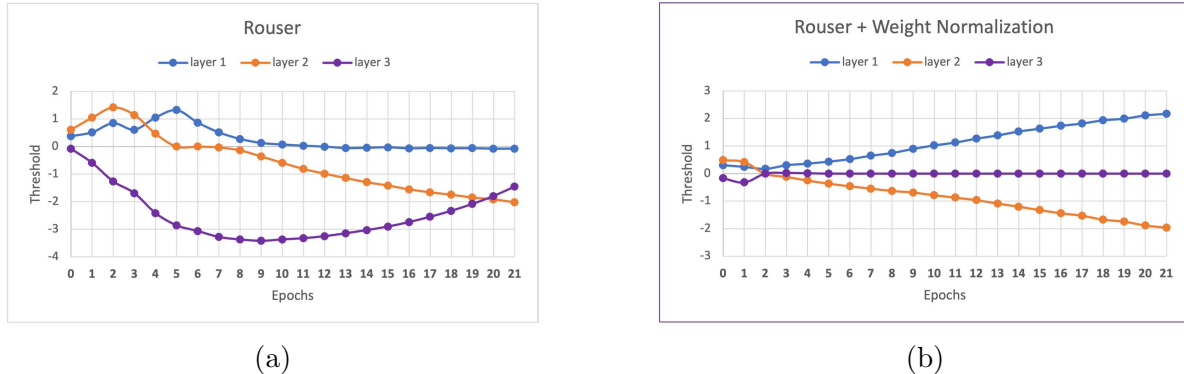


Figure 7: Tracking dynamic threshold values for NMNIST as neurons in each layer have an initial threshold value of 0.25 and adapt to input changes during training with Rouser.

Table 3: Percentage of “dead neurons” during training on NMNIST, where layers 1 and 2 have 500 neurons and layer 3 has 10 neurons.

Training method	Layer 1	Layer 2	Layer 3
Slayer 2.0	45.6%	61.8%	76.4%
Rouser	37.1%	15.4%	0%

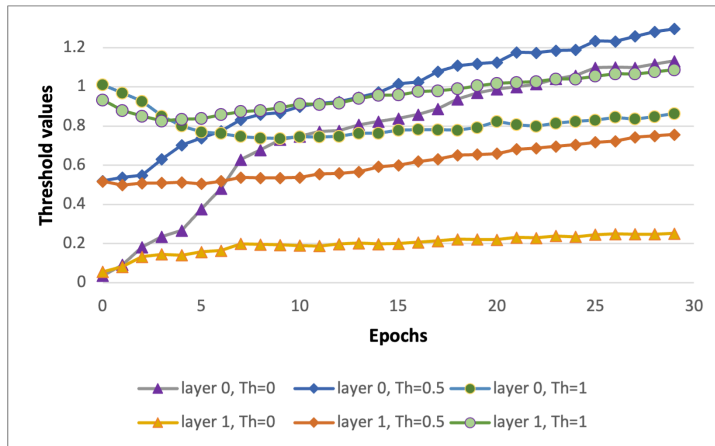


Figure 8: Tracking dynamic threshold values for DVS128 as neurons in each layer start with initial threshold values of 0, 0.5, and 1, and adapt to input changes during training with Rouser.

We conducted a further investigation into Rouser by examining the neuron activities in the network during training. We observed a lower count of “dead neurons” in Rouser than in SLAYER 2.0 (see Table 3). By dynamically adapting the threshold levels, Rouser enables a greater number of neurons to generate spikes and actively participate in error backpropagation throughout the training process. When the threshold level is high and neurons operate in a sub-threshold region, they have a near-zero gradient, and don’t emit any spikes. This results in the neurons remaining dead and, consequently, unable to contribute to the learning process. Additionally, in Figure 9 we provide a comparison of the percentage of spikes emitted during inference relative to the maximum number of spikes possible for each layer. Rouser demonstrates more effective spike regulation in the SNN network. It initially exhibits a higher spike rate in layers 1 and 2, but as the network settles, it demonstrates fewer spikes than SLAYER 2. The loss function is calculated after layer 3; therefore, the winning neuron in this layer will try match the desired target spike train for both methods, which will have spikes for over half of the time (at least 150 spikes in NMNIST with time interval of 300).

In Figure 10, we show the percentage of active neurons per layer over time during training. We observed in Figure 10c that all neurons in the output layer (Layer 3) remained silent during the initial stages of training with SLAYER 2.0 (epochs 0 to 5). This lack of activity in the output layer contributes to slower training previously depicted

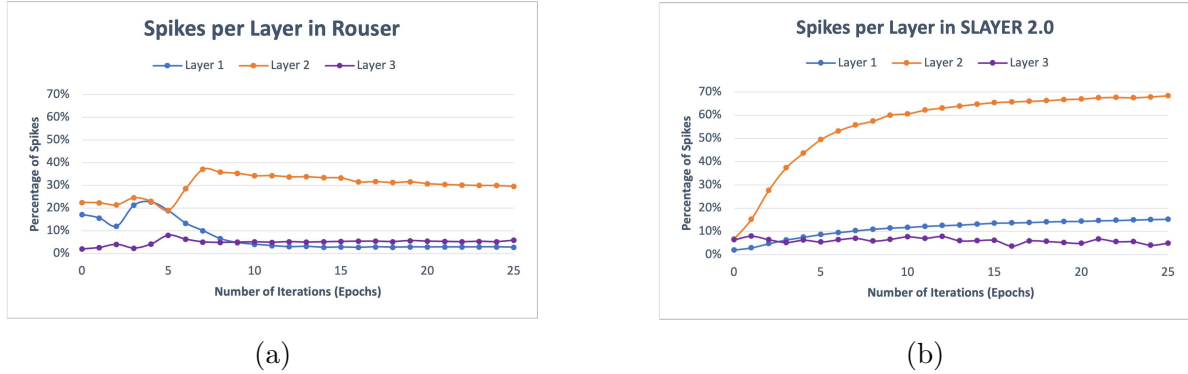


Figure 9: Percentage of spikes emitted during inference on NMNIST relative to the maximum number of spikes. In layers 1 and 2, the maximum number of spikes possible is 500×300 . For layer 3, this number is 10×300 .

in Figures 4b and 5b. In Figure 10b, we observed that adding weight normalization to SLAYER 2.0 led to an escalation in the number of active neurons starting from epoch 5. Note, however, that weight normalization leads to a considerable slowdown in (wall clock) training speed due to its computational overhead. In Figure 10a, through the adjustment of threshold values, Rouser achieved a remarkable increase in the number of active neurons in layer 3 to 100%. This indicates that all neurons in the output layer were actively participating in spike generation and contributing to the gradient backpropagation process during training. Rouser successfully activated all previously dead neurons in the output layer, resulting in a noticeable improvement in both latency and accuracy.

4.2. Ablation Studies

We conducted an ablation study to meticulously investigate the isolated influence of adaptive thresholding in Rouser, while excluding the effects of other parameters. In this study, we set the threshold learning rate to zero and simultaneously disabled weight normalization, while retaining all other parameters, including weight initialization scheme, unchanged. In addition, we enforced the use of the same initial weights across experiments. We conducted this study under two sub-optimal hyperparameter settings where Rouser exhibited improved accuracy (Figure 11a) and enhanced training stability (Figure 11b). In Figure 11b, we observed that not adjusting the threshold (threshold learning rate of zero) resulted in an inability to learn. Even a threshold learning rate of 0.001 failed to produce significant learning. This necessitated a higher threshold learning rate of 0.01 to induce learning in neurons.

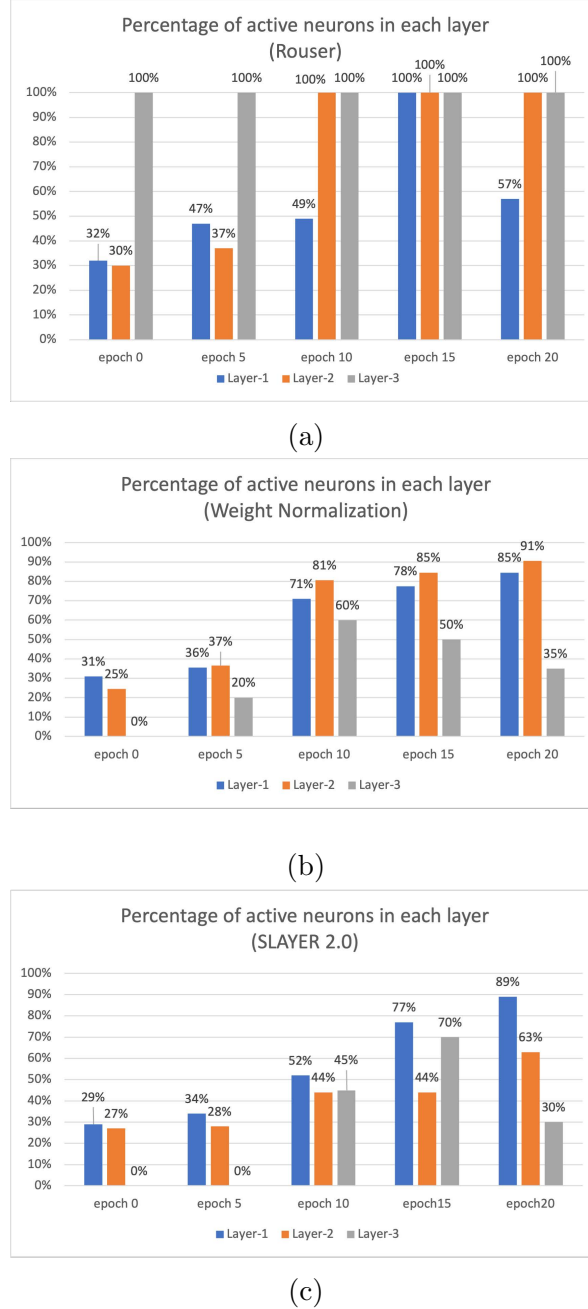


Figure 10: The percentage of active neurons (neurons emitting at least one spike) in each layer during training. Numbers represent the values for the first input data in the last training batch, and they have been averaged across three runs.

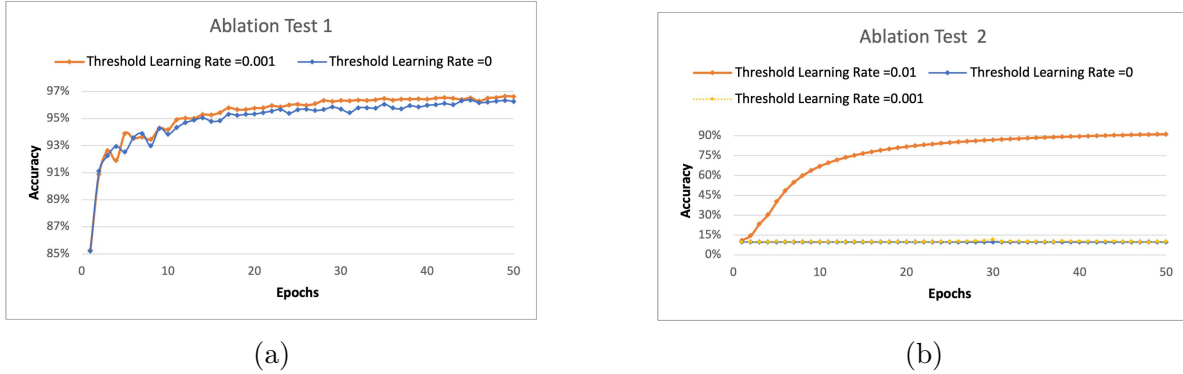


Figure 11: Ablation studies on NMNIST for sub-optimal hyperparameters (Th_{init} , τ , s) = (1.25, 3.75, 1.5) in (a), and (0.25, 3, 3) in (b). Note: Threshold rate 0 and 0.001 data are very similar over this range and the plots overlap substantially.

5. Conclusion

This work presents Rouser, a method for adaptively setting the threshold of neurons in an SNN during training, sensitive to input dynamism, in order to “rouse” dead neurons. By experimenting with three datasets, MNIST, DVS128 and SHD, we demonstrate the effectiveness of this technique in improving network performance in terms of training latency and testing accuracy and show how Rouser’s adaptive firing thresholds achieve consistently high accuracy and robustness to variation in initial hyperparameters. Rouser achieves its goal of greatly mitigating the number of dead neurons during training while actually improving activation sparsity during testing, improving overall accuracy, and reducing the time to initial model convergence compared to state of the art SNN training techniques.

References

- [1] Misha Mahowald. *The Silicon Retina*, pages 4–65. Springer US, Boston, MA, 1994.
 - [2] L. Watts, D.A. Kerns, R.F. Lyon, and C.A. Mead. Improved implementation of the silicon cochlea. *IEEE Journal of Solid-State Circuits*, 27(5):692–700, 1992.
 - [3] Yu Nishitani, Yukihiro Kaneko, and Michihito Ueda. Supervised learning using spike-timing-dependent plasticity of memristive synapses. *IEEE Transactions on Neural Networks and Learning Systems*, 26(12):2999–3008, 2015.
 - [4] Patrick M Sheridan, Fuxi Cai, Chao Du, Wen Ma, Zhengya Zhang, and Wei D Lu. Sparse coding with memristor networks. *Nature Nanotechnology*, 12(8):784–789, 2017.
 - [5] Dmitri B Strukov, Gregory S Snider, Duncan R Stewart, and R Stanley Williams. The missing memristor found. *Nature*, 453(7191):80–83, 2008.
 - [6] Filipp Akopyan, Jun Sawada, Andrew Cassidy, Rodrigo Alvarez-Icaza, John V. Arthur, Paul Merolla, Nabil Imam, Yutaka Y. Nakamura, Pallab Datta, Gi-Joon Nam, Brian Taba, Michael Beakes, Bernard Brezzo, Jente B. Kuang, Rajit Manohar, William P. Risk, Bryan L. Jackson, and Dharmendra S. Modha. Truenorth: Design and tool flow of a 65 mw 1 million neuron programmable neurosynaptic chip. *IEEE Trans. on CAD of Integrated Circuits and Systems*, 34(10):1537–1557, 2015.

- [7] Sebastian Höppner, Yexin Yan, Andreas Dixius, Stefan Scholze, Johannes Partzsch, Marco Stolba, Florian Kelber, Bernhard Vogginger, Felix Neumärker, Georg Ellguth, et al. The spinnaker 2 processing element architecture for hybrid digital neuromorphic computing. *arXiv preprint arXiv:2103.08392*, 2021.
- [8] Mike Davies, Narayan Srinivasa, Tsung-Han Lin, Gautham Chinya, Yongqiang Cao, Sri Harsha Choday, Georgios Dimou, Prasad Joshi, Nabil Imam, Shweta Jain, et al. Loihi: A neuromorphic manycore processor with on-chip learning. *IEEE Micro*, 38(1):82–99, 2018.
- [9] Brainchip. Akida Neural Processor. <https://www.brainchip.com/technology>. Accessed: April 2024.
- [10] GrAI Matter Labs. <https://www.graimatterlabs.ai/technology>. Accessed: April 2024.
- [11] Travis DeWolf, Paweł Jaworski, and Chris Eliasmith. Nengo and low-power ai hardware for robust, embedded neurorobotics. *Frontiers in Neurorobotics*, 14, 2020.
- [12] Guillermo Gallego, Tobi Delbrück, Garrick Orchard, Chiara Bartolozzi, Brian Taba, Andrea Censi, Stefan Leutenegger, Andrew J. Davison, Jörg Conradt, Kostas Daniilidis, and Davide Scaramuzza. Event-based vision: A survey. *IEEE Transactions on Pattern Analysis and Machine Intelligence*, 44(1):154–180, 2022.
- [13] M. Litzenberger, B. Kohn, A.N. Belbachir, N. Donath, G. Gritsch, H. Garn, C. Posch, and S. Schraml. Estimation of vehicle speed based on asynchronous data from a silicon retina optical sensor. In *2006 IEEE Intelligent Transportation Systems Conference*, pages 653–658, 2006.
- [14] Yulia Sandamirskaya, Mohsen Kaboli, Jorg Conradt, and Tansu Celikel. Neuromorphic computing hardware and neural architectures for robotics. *Science Robotics*, 7(67):eabl8419, 2022.
- [15] Guangzhi Tang, Arpit Shah, and Konstantinos P Michmizos. Spiking neural network on neuromorphic hardware for energy-efficient unidimensional slam. In *2019 IEEE/RSJ International Conference on Intelligent Robots and Systems (IROS)*, pages 4176–4181. IEEE, 2019.
- [16] Richard Kempter, Wulfram Gerstner, and J Leo Van Hemmen. Hebbian learning and spiking neurons. *Physical Review E*, 59(4):4498, 1999.
- [17] Sen Song, Kenneth D Miller, and Larry F Abbott. Competitive hebbian learning through spike-timing-dependent synaptic plasticity. *Nature Neuroscience*, 3(9):919–926, 2000.
- [18] Peter U Diehl and Matthew Cook. Unsupervised learning of digit recognition using spike-timing-dependent plasticity. *Frontiers in Computational Neuroscience*, 9:99, 2015.
- [19] Paul Ferré, Franck Mamalet, and Simon J Thorpe. Unsupervised feature learning with winner-takes-all based stdp. *Frontiers in Computational Neuroscience*, 12:24, 2018.
- [20] H. Sebastian Seung. Learning in spiking neural networks by reinforcement of stochastic synaptic transmission. *Neuron*, 40(6):1063–1073, 2003.
- [21] Ronald J Williams. Simple statistical gradient-following algorithms for connectionist reinforcement learning. *Machine Learning*, 8:229–256, 1992.
- [22] Yongqiang Cao, Yang Chen, and Deepak Khosla. Spiking deep convolutional neural networks for energy-efficient object recognition. *International Journal of Computer Vision*, 113:54–66, 2015.
- [23] Peter U. Diehl, Daniel Neil, Jonathan Binas, Matthew Cook, Shih-Chii Liu, and Michael Pfeiffer. Fast-classifying, high-accuracy spiking deep networks through weight and threshold balancing. In *2015 International Joint Conference on Neural Networks (IJCNN)*, pages 1–8, 2015.
- [24] Nitin Rathi and Kaushik Roy. Diet-snn: A low-latency spiking neural network with direct input encoding and leakage and threshold optimization. *IEEE Transactions on Neural Networks and Learning Systems*, 34(6):3174–3182, 2023.
- [25] Abhronil Sengupta, Yuting Ye, Robert Wang, Chiao Liu, and Kaushik Roy. Going deeper in spiking neural networks: Vgg and residual architectures. *Frontiers in Neuroscience*, 13:95, 2019.
- [26] Nicolas Perez-Nieves and Dan Goodman. Sparse spiking gradient descent. *Advances in Neural Information Processing Systems (NeurIPS)*, 34:11795–11808, 2021.

- [27] Sander M Bohte, Joost N Kok, and Johannes A La Poutré. Spikeprop: backpropagation for networks of spiking neurons. In *ESANN*, volume 48, pages 419–424. Bruges, 2000.
- [28] Sumit B Shrestha and Garrick Orchard. Slayer: Spike layer error reassignment in time. *Advances in Neural Information Processing Systems (NeurIPS)*, 31, 2018.
- [29] Friedemann Zenke and Surya Ganguli. Superspike: Supervised learning in multilayer spiking neural networks. *Neural Computation*, 30(6):1514–1541, 2018.
- [30] Jun Haeng Lee, Tobi Delbrück, and Michael Pfeiffer. Training deep spiking neural networks using backpropagation. *Frontiers in Neuroscience*, 10:508, 2016.
- [31] Jacques Kaiser, Hesham Mostafa, and Emre Neftci. Synaptic plasticity dynamics for deep continuous local learning (decolle). *Frontiers in Neuroscience*, 14:424, 2020.
- [32] Emre O. Neftci, Hesham Mostafa, and Friedemann Zenke. Surrogate gradient learning in spiking neural networks: Bringing the power of gradient-based optimization to spiking neural networks. *IEEE Signal Processing Magazine*, 36(6):51–63, 2019.
- [33] Friedemann Zenke and Tim P Vogels. The remarkable robustness of surrogate gradient learning for instilling complex function in spiking neural networks. *Neural Computation*, 33(4):899–925, 2021.
- [34] Geoffrey Hinton. The forward-forward algorithm: Some preliminary investigations, 2022.
- [35] Gina G Turrigiano and Sacha B Nelson. Homeostatic plasticity in the developing nervous system. *Nature reviews neuroscience*, 5(2):97–107, 2004.
- [36] Bojian Yin, Federico Corradi, and Sander M Bohté. Effective and efficient computation with multiple-timescale spiking recurrent neural networks. In *International Conference on Neuromorphic Systems 2020*, pages 1–8, 2020.
- [37] Ahmed Shaban, Sai Sukruth Bezugam, and Manan Suri. An adaptive threshold neuron for recurrent spiking neural networks with nanodevice hardware implementation. *Nature Communications*, 12(1):4234, 2021.
- [38] Guillaume Bellec, Darjan Salaj, Anand Subramoney, Robert Legenstein, and Wolfgang Maass. Long short-term memory and learning-to-learn in networks of spiking neurons. *Advances in Neural Information Processing Systems (NeurIPS)*, 31, 2018.
- [39] Darjan Salaj, Anand Subramoney, Ceca Krajsnikovic, Guillaume Bellec, Robert Legenstein, and Wolfgang Maass. Spike frequency adaptation supports network computations on temporally dispersed information. *eLife*, 10:e65459, jul 2021.
- [40] Jason Kamran Eshraghian and Wei D. Lu. The fine line between dead neurons and sparsity in binarized spiking neural networks. *CoRR*, abs/2201.11915, 2022.
- [41] Siqi Wang, Tee Hiang Cheng, and Meng-Hiot Lim. Ltmd: learning improvement of spiking neural networks with learnable thresholding neurons and moderate dropout. *Advances in Neural Information Processing Systems (NeurIPS)*, 35:28350–28362, 2022.
- [42] Wei Fang, Zhaofei Yu, Yanqi Chen, Timothée Masquelier, Tiejun Huang, and Yonghong Tian. Incorporating learnable membrane time constant to enhance learning of spiking neural networks. In *Proceedings of the IEEE/CVF International Conference on Computer Vision*, pages 2661–2671, 2021.
- [43] Larry F Abbott. Lapicque’s introduction of the integrate-and-fire model neuron (1907). *Brain Research Bulletin*, 50(5-6):303–304, 1999.
- [44] Mark CW van Rossum. A novel spike distance. *Neural Computation*, 13(4):751–763, 2001.
- [45] Giacomo Indiveri, Bernabé Linares-Barranco, Tara Julia Hamilton, André van Schaik, Ralph Etienne-Cummings, Tobi Delbrück, Shih-Chii Liu, Piotr Dudek, Philipp Häfliger, Sylvie Renaud, et al. Neuromorphic silicon neuron circuits. *Frontiers in Neuroscience*, 5:73, 2011.
- [46] Maurizio Mattia and Paolo Del Giudice. Efficient event-driven simulation of large networks of spiking neurons and dynamical synapses. *Neural Computation*, 12(10):2305–2329, 2000.
- [47] Diederik P Kingma and Jimmy Ba. Adam: A method for stochastic optimization. *arXiv preprint arXiv:1412.6980*, 2014.
- [48] Geoffrey Hinton, Nitish Srivastava, and Kevin Swersky. Neural networks for machine learning

- lecture 6a overview of mini-batch gradient descent. *Cited on*, 14(8):2, 2012.
- [49] Garrick Orchard, Ajinkya Jayawant, Gregory K Cohen, and Nitish Thakor. Converting static image datasets to spiking neuromorphic datasets using saccades. *Frontiers in Neuroscience*, 9:437, 2015.
 - [50] Arnon Amir, Brian Taba, David Berg, Timothy Melano, Jeffrey McKinstry, Carmelo Di Nolfo, Tapan Nayak, Alexander Andreopoulos, Guillaume Garreau, Marcela Mendoza, et al. A low power, fully event-based gesture recognition system. In *Proceedings of the IEEE conference on Computer Vision and Pattern Recognition*, pages 7243–7252, 2017.
 - [51] Benjamin Cramer, Yannik Stradmann, Johannes Schemmel, and Friedemann Zenke. The heidelberg spiking data sets for the systematic evaluation of spiking neural networks. *IEEE Transactions on Neural Networks and Learning Systems*, 33(7):2744–2757, 2020.
 - [52] Gregory K Cohen, Garrick Orchard, Sio-Hoi Leng, Jonathan Tapson, Ryad B Benosman, and André Van Schaik. Skimming digits: neuromorphic classification of spike-encoded images. *Frontiers in Neuroscience*, 10:184, 2016.
 - [53] Bharath Ramesh, Hong Yang, Garrick Orchard, Ngoc Anh Le Thi, Shihao Zhang, and Cheng Xiang. Dart: distribution aware retinal transform for event-based cameras. *IEEE Transactions on Pattern Analysis and Machine Intelligence*, 42(11):2767–2780, 2019.
 - [54] Intel. Lava software framework. <https://lava-nc.org/>. Accessed: September 2023.
 - [55] Tim Salimans and Durk P Kingma. Weight normalization: A simple reparameterization to accelerate training of deep neural networks. *Advances in Neural Information Processing Systems (NeurIPS)*, 29, 2016.